

Journal Pre-proof

Novel method for the production of copper(II) formates, their thermal, spectral and magnetic properties

V.N. Krasil'nikov, V.P. Zhukov, E.V. Chulkov, I.V. Baklanova, D.G. Kellerman, O.I. Gyrdasova, T.V. Dyachkova, A.P. Tyutyunnik



PII: S0925-8388(20)32572-X

DOI: <https://doi.org/10.1016/j.jallcom.2020.156208>

Reference: JALCOM 156208

To appear in: *Journal of Alloys and Compounds*

Received Date: 8 April 2020

Revised Date: 7 June 2020

Accepted Date: 24 June 2020

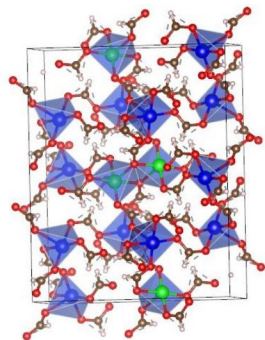
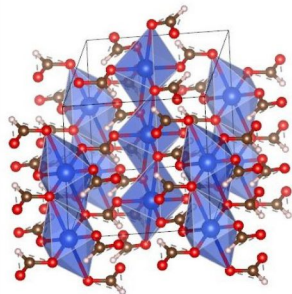
Please cite this article as: V.N. Krasil'nikov, V.P. Zhukov, E.V. Chulkov, I.V. Baklanova, D.G. Kellerman, O.I. Gyrdasova, T.V. Dyachkova, A.P. Tyutyunnik, Novel method for the production of copper(II) formates, their thermal, spectral and magnetic properties, *Journal of Alloys and Compounds* (2020), doi: <https://doi.org/10.1016/j.jallcom.2020.156208>.

This is a PDF file of an article that has undergone enhancements after acceptance, such as the addition of a cover page and metadata, and formatting for readability, but it is not yet the definitive version of record. This version will undergo additional copyediting, typesetting and review before it is published in its final form, but we are providing this version to give early visibility of the article. Please note that, during the production process, errors may be discovered which could affect the content, and all legal disclaimers that apply to the journal pertain.

© 2020 Published by Elsevier B.V.

V.N. Krasil'nikov: Conceptualization, Investigation, Roles/Writing - original draft, Writing - review & editing, **V.P. Zhukov:** Investigation, Formal analysis, Writing - review & editing, **E.V. Chulkov:** Formal analysis, **I.V. Baklanova:** Investigation, Visualization, Formal analysis, **D.G. Kellerman:** Investigation, Visualization, Formal analysis, **O.I. Gyrdasova:** Formal analysis, **T.V. Dyachkova:** Formal analysis, **A.P. Tyutyunnik:** Investigation, Visualization, Formal analysis.

Journal Pre-proof

 α -Cu(HCOO)₂ β -Cu(HCOO)₂

Journal Pre-proof

Novel method for the production of copper(II) formates, their thermal, spectral and magnetic properties

V.N. Krasil'nikov¹, V.P. Zhukov¹, E.V. Chulkov^{2,3,4,5}, I.V. Baklanova¹, D.G. Kellerman¹,
O.I. Gyrdasova¹, T.V. Dyachkova¹, A.P. Tyutyunnik¹

¹Institute of Solid State Chemistry Ural Branch Russian Academy Science, Ekaterinburg, Russia

²Departamento de Física de Materiales Universidad del País VascoUPV/EHU, San Sebastián/Donostia, Spain

³Donostia International Physics Center (DIPC), San Sebastián/Donostia, Spain

⁴Saint Petersburg State University, Saint Petersburg, Russia

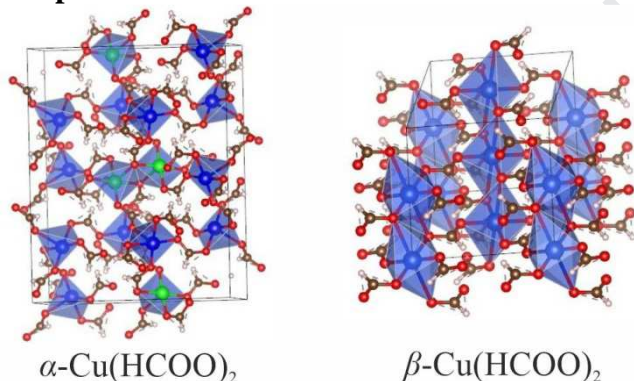
⁵Tomsk State University, Tomsk, Russia

Abstract

A new method for the synthesis of various types of copper(II) formates with $\text{Cu}(\text{NO}_3)_2 \cdot 3\text{H}_2\text{O}$ and formic acid, orthorhombic (α) and monoclinic (β) modifications of anhydrous copper(II) formate, as well as $\text{Cu}(\text{HCOO})_2 \cdot 2\text{H}_2\text{O}$ and $\text{Cu}(\text{HCOO})_2 \cdot 4\text{H}_2\text{O}$. The identity of the obtained compounds was confirmed by X-ray phase analysis, optical microscopy and thermogravimetry methods. It was shown that $\text{Cu}(\text{HCOO})_2 \cdot 4\text{H}_2\text{O}$ can be used as a precursor for producing copper powders with particle size of the order of 150 nm. The results of investigation of vibration and absorption spectra of α and β modifications of anhydrous copper(II) formate are presented. Their magnetic behavior in the temperature interval 2-300 K was estimated, and comparative analysis of magnetic properties was carried out. First-principle calculations of electronic band structure for anhydrous α and β modifications were performed. The results obtained correspond to experimentally observed structural instability of β - $\text{Cu}(\text{HCOO})_2$, fundamental absorption edge enhancement during transition from α to β modification, and low-temperature ferromagnetic ordering in α - $\text{Cu}(\text{HCOO})_2$. Simulation for β modification is indicative of antiferromagnetic ordering of magnetic moments inside chains formed by copper-oxygen octahedra.

Keywords: formate, copper(II), UV-Vis-NIR spectra, IR spectra, magnetic properties, first-principle calculations

Graphical abstract



Introduction

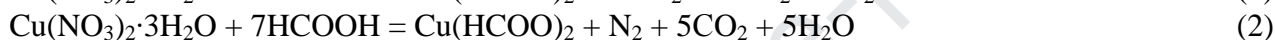
Much attention was focused recently on bivalent copper(II) formates of the general composition $\text{Cu}(\text{HCOO})_2 \cdot n\text{H}_2\text{O}$ ($n = 0, 2, 4$) due to the prospects of their application as precursors in technologies for producing different functional materials, for example, molecular magnets – perovskite-like organometallic compounds with framework structure, complex oxides, ultradispersed copper powders, films, profile contacts, deposited catalysts, metalloorganic inks and polymeric composite materials for various electronic devices [1-16,17]. The wide range of promising practical applications of copper(II) formates is determined by their pronounced ability to transform into metal (Cu^0) on heating in inert gaseous atmosphere without formation of impurities of organic polymers and elementary carbon [11,12,18-21] which is typical for compounds of higher carboxylic acids, for example, succinate, maleate etc. [22-26]. The development of methods for the synthesis of copper nanoparticles with controllable dimensions, shape and surface properties is of much importance for their application in various fields of nanotechnology where gold, silver and platinum nanoparticles are already traditionally used at present [27,28]. Besides, copper(II) formates themselves are known to possess interesting magnetic and dielectric properties [18, 29-33]. Presently, $\text{Cu}(\text{HCOO})_2$ [30, 32], $\text{Cu}(\text{HCOO})_2 \cdot 2\text{H}_2\text{O}$ [34-36], $\text{Cu}(\text{HCOO})_2 \cdot 4\text{H}_2\text{O}$ [31,37-39] have been fairly well studied and described in the scientific literature. Anhydrous copper(II) formate exists in three structural modifications, among which α - $\text{Cu}(\text{HCOO})_2$ (orthorhombic) and β - $\text{Cu}(\text{HCOO})_2$ (monoclinic) [19, 32, 33] are stable under usual conditions. Considering the importance of

copper(II) formates as reagents and functional materials, effective approaches to their synthesis are being actively developed. Currently, the familiar synthesis methods are based on the interaction of formic acid with CuO, Cu(OH)₂ and Cu₂(OH)₂CO₃ in aqueous medium [11,18-21,31-39]. Most of these methods are complicated multistage processes aimed at synthesis of a specific compound by selecting a copper-containing precursor, formic acid concentration, reaction medium, conditions of reagents interaction and crystallization of products. Poorly crystallized anhydrous copper(II) formate can be also produced in the form of monoclinic β modification by dehydration of Cu(HCOO)₂·4H₂O [32,39]. In our work we have developed and implemented a universal and technologically simple method for copper(II) formate synthesis allowing α -Cu(HCOO)₂, β -Cu(HCOO)₂, Cu(HCOO)₂·2H₂O and Cu(HCOO)₂·4H₂O to be obtained. For the purpose of chemical and structural identification and research of physicochemical properties of compounds synthesized by the developed technology, we employed X-ray diffraction (XPA), optical and electron microscopy, thermogravimetry (DTA and TG analysis), vibration and absorption spectroscopy, and magnetometry methods. The experimental results of magnetic properties investigations were compared with the first-principles calculation data. The primary focus was on the examination of anhydrous modifications of copper(II) formate as the most stable ones under real conditions.

Experiment technique

1. Synthesis

The process simplicity and universal character of the developed method for the synthesis of copper(II) formates are provided by the use of Cu(NO₃)₂·3H₂O as a source of copper(II), which is highly soluble in formic acid at room temperature irrespective of its concentration. The interaction of reagents is described by the following reactions:



Reaction (1) proceeds with the use of concentrated formic acid, it begins spontaneously at room temperature and is accompanied by strong heating (up to ~100 °C) and intensive emission of brown vapors of nitrogen dioxide. The interaction according to reaction (2) takes place with weak heating of copper(II) nitrate solution in diluted formic acid, the major part of which is used to reduce nitrate ion to molecular nitrogen by reaction [40]:



Considering the probabilities of reactions (1 and 2) in the system copper nitrate – formic acid, the following options of copper(II) formates synthesis were proposed.

Synthesis of monoclinic β modification of anhydrous copper(II) formate. A powder of copper nitrate of the composition Cu(NO₃)₂·3H₂O in the amount of 2.5 g was dissolved in 3.0 ml of 99.7% formic acid HCOOH at room temperature. The interaction begins spontaneously after dissolution of nitrate and is accompanied by strong heating and formation of blue crystals, whose X-ray diffraction pattern (**Fig. 1S**) corresponds to β -Cu(HCOO)₂ with lattice parameters: $a = 8.1998(8)$, $b = 7.9337(7)$, $c = 3.6266(2)$ Å, $\beta = 122.17(1)^\circ$, $V = 199.71$ Å³. Under the microscope, β -Cu(HCOO)₂ crystals are observed mainly as oblique extended plates with refractive indices: Ng = 1.722, Nm = 1.681, Np = 1.630.

Synthesis of orthorhombic α modification of anhydrous copper(II) formate. 2.5 g of copper nitrate Cu(NO₃)₂·3H₂O powder were dissolved in 3.0 ml of 99.7% formic acid HCOOH at room temperature. β -Cu(HCOO)₂ crystals were formed whereupon 1 ml of distilled water was added and heated at 80 °C until blue color of the deposit changed to dark blue, which according to XPA data (**Fig. 2S**) was due to the formation of orthorhombic α modification of anhydrous copper formate with lattice parameters: $a = 14.203(1)$, $b = 8.9441(8)$, $c = 6.2305(7)$ Å, $V = 791.48$ Å³. Under the microscope, dark blue crystals in the form of needles and elongated plates with refractive indices: Ng = 1.689, Nm = 1.643, Np = 1.597 were observed. Synthesis of α -Cu(HCOO)₂ without passing through the stage of β -Cu(HCOO)₂ formation is possible, for example, by mixing Cu(NO₃)₂·3H₂O with 70% formic acid and heating the mixture at 60-80 °C.

Synthesis of monoclinic modification of copper(II) formate dihydrate. Copper nitrate Cu(NO₃)₂·3H₂O powder taken in the amount of 2.5 g was dissolved in 50 ml of 20% formic acid HCOOH at a temperature of 50 °C. The solution was evaporated until a greenish-blue deposit was formed, which was separated by vacuum filtration, dried at room temperature and placed into an airtight vessel for storage. According to XPA data (**Fig. 3S**), a monoclinic modification of copper formate of the composition Cu(HCOO)₂·2H₂O with lattice parameters: $a = 8.5190(8)$, $b = 7.1346(7)$, $c = 9.439(1)$ Å, $\beta = 96.91(2)^\circ$, $V = 569.53$ Å³ is formed. Cu(HCOO)₂·2H₂O crystals have a form of hexagonal plates with refractive indices: Ng = 1.591, Nm = 1.540,

$N_p = 1.518$. The color of β -Cu(HCOO)₂, α -Cu(HCOO)₂ and Cu(HCOO)₂·2H₂O powders is demonstrated in the photographic images in **Fig. 4S**.

Synthesis of monoclinic modification of copper(II) formate tetrahydrate. 2.5 g of copper nitrate Cu(NO₃)₂·3H₂O were dissolved in 50 ml of 20% formic acid HCOOH at 50 °C. The produced solution was kept open at room temperature until large light blue crystals were deposited (**Fig. 5S**). According to XPA data, in this case a monoclinic modification of copper(II) formate of the composition Cu(HCOO)₂·4H₂O with lattice parameters: $a = 8.1480(9)$, $b = 8.1318(9)$, $c = 6.3053(7)$ Å, $\beta = 100.79(2)^\circ$, $V = 410.39$ Å³ is formed.

2. Instrumentation

The phase analysis of the precursors and the products of their thermolysis was carried out with the use of a POLAM S-112 polarizing microscope in transmitted light (the refractive indices were determined by the immersion method at room temperature) and a STADI-P automatic X-ray powder diffractometer (STOE, Germany) in CuK _{α 1}-radiation using the powder diffraction file PDF-2 (ICDD Release 2016). The thermal analysis was performed on a SETARAM Setsys Evolution thermoanalyzer during heating in air with a rate of 10 °C·min⁻¹. The morphological features were examined using the scanning electron microscopy (SEM) method on a JEOLJSM 6390 LA microscope (magnification factor 5-300000, resolving power 3.0 nm at 20 kV). The IR spectra were collected on a Vertex 80 IR Fourier spectrometer (Bruker) in the interval of 4000-400 cm⁻¹ from powder-like samples palletized with CsI. IR spectra in the 4000-360 cm⁻¹ range were recorded on a Vertex 80 (Bruker) spectrometer using MVP-Pro ATR Accessory with diamond crystal (Harrick). The UV-Vis-NIR spectra were recorded in the interval 190-1300 nm on a UV-2600 (Shimadzu) spectrometer using BaSO₄ as standard. The magnetic properties were studied for a powder sample with the use of a vibrating sample magnetometer VSM-5T (Cryogenic Ltd.). The temperature dependences of DC magnetization M were measured in the temperature interval from 2 to 300 K. The magnetization curves were measured at 2 K and 300 K in magnetic fields to 5 T.

Results and discussion

1. Experimental results and discussion

The data of thermogravimetric analysis of two modifications of anhydrous copper(II) formate and dehydrate are presented in Figs. 1-3 as TG and DTA curves. Thermal decomposition of α -Cu(HCOO)₂ and β -Cu(HCOO)₂ is an exothermic process as evidenced by the maxima on the DTA curves (Figs. 1 and 2). The mass loss of the samples heated in air to 500 °C is estimated from the TG curves to be 48.26% (Fig. 1) and 48.04% (Fig. 2), which corresponds to the calculated value 48.19% provided that copper(II) oxide CuO is formed. The mass loss in the minimum points on the TG curves at 223 and 236 °C ($\sim\Delta m = 54$ %) corresponds to the formation of copper(I) oxide Cu₂O during decomposition of α - and β -Cu(HCOO)₂ ($\Delta m = 53.40$ %), whose oxidation determines the samples' mass enhancement with further increase in temperature.

The formation of crystalline hydrate Cu(HCOO)₂·2H₂O is confirmed by the TG and DTA curves (Fig. 3). The mass loss of the sample at 120 °C is 18.53 mass%, which corresponds to the estimated data ($\Delta m = 18.99$ %) provided that two moles of H₂O are removed. The decomposition of the dehydration product also proceeds with heat release and according to mass-spectrometry data is accompanied by isolation of H₂O and CO₂ (Fig. 3). The thermal properties of copper(II) formate tetrahydrate were not studied by DTA and TG methods because of its extremely low stability in ambient conditions: this compound decomposes into Cu(HCOO)₂·2H₂O and β -Cu(HCOO)₂ already at room temperature during preparation. In the cause of time, a light blue deposit of small β -Cu(HCOO)₂ crystals is formed on the surface of large crystals Cu(HCOO)₂·4H₂O due to their exposure in an open vessel. According to XPA data (**Fig. 6S**), upon one day exposure in an open vessel the sample of Cu(HCOO)₂·4H₂O contains 50.9 mass% of initial phase, 38.3 mass% of Cu(HCOO)₂·2H₂O and 10.8 mass% of β -Cu(HCOO)₂. However, on heating to 500 °C the mass loss of freshly prepared Cu(HCOO)₂·4H₂O sample is 64.12 mass%, which agrees well with the estimated data ($\Delta m = 64.73$ mass%) for its decomposition with the formation of copper oxide CuO. According to earlier studies [38], the water loss for Cu(HCOO)₂·4H₂O corresponds to four H₂O molecules per formula unit and proceeds in one stage without intermediate formation of dehydrate during both isothermal dehydration at 50 °C and continuous heating to 110 °C, when anhydrous monoclinic β modification of copper(II) formate is formed. On the other hand, the authors of work [41] showed with the use of thermogravimetric and X-ray phase analysis methods that the process of dehydration of Cu(HCOO)₂·4H₂O during heating in air takes place in two stages with successive formation of Cu(HCOO)₂·2H₂O and β -Cu(HCOO)₂.

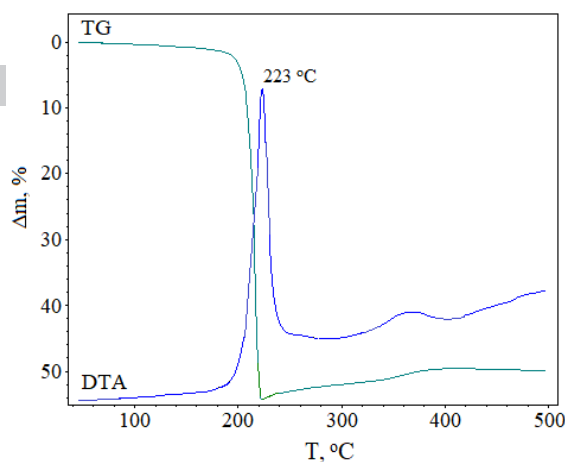


Fig. 1. TG and DTA curves for α -Cu(HCOO)₂.

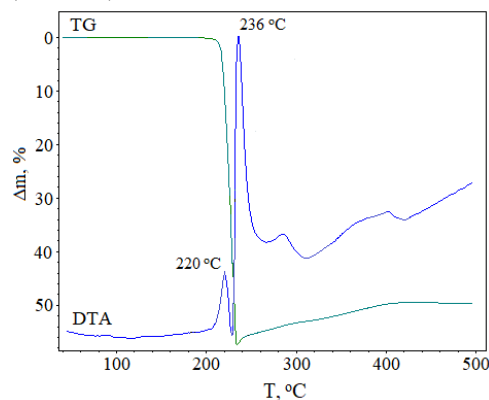


Fig. 2. TG and DTA curves for β -Cu(HCOO)₂.

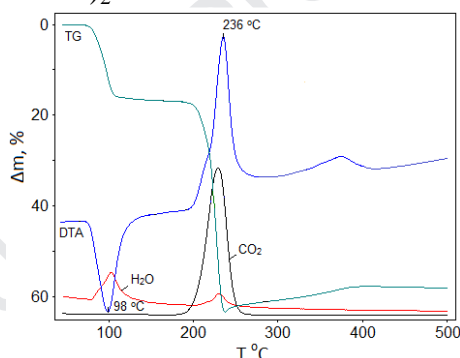


Fig. 3. TG, DTA curves and mass-spectrometry data for Cu(HCOO)₂·2H₂O.

Thus, all the synthesized copper(II) formates are transformed into CuO during heating in air to 500 °C at a rate of 10 °C/min. The minima observed on the TG curves are due apparently to the formation of copper in the form of oxide Cu₂O and metal Cu⁰ [26], whose transformation into CuO corresponds to enhancement and stabilization of the sample mass at temperatures above 400 °C (Figs. 1-3). According to data of works [11, 18-21], Cu(HCOO)₂ decomposes with the formation of elemental copper on heating in inert gaseous atmosphere. The process occurs at low temperatures and is accompanied by release of H₂, CO and CO₂ creating conditions for preserving copper in the form of metal [7,20]. Figure 4 displays the photographic images of Cu(HCOO)₂·4H₂O crystal and aggregates CuO and Cu⁰ formed as a result of its decomposition at 400 °C in air and in helium atmosphere, respectively. It is seen that the aggregates of thermolysis products, in spite of dramatic changes in the composition, preserve the appearance of Cu(HCOO)₂·4H₂O crystal. The SEM images in Fig. 5 demonstrate that the aggregates of the products of Cu(HCOO)₂·4H₂O thermolysis in air and in helium atmosphere actually have a loose internal structure and consist of CuO (Fig. 5a) and Cu⁰ (Fig. 5b) particles with average size of about 150 nm. These aggregates easily decompose into constituent particles on exposure to mechanical action or ultrasound. Figure 6 shows the morphology of the aggregates of the products of α -Cu(HCOO)₂ thermolysis in air and in helium atmosphere at 400 °C. In this case, the decomposition of anhydrous copper(II) formate gives rise to more dense aggregates built of CuO (Fig. 6a) and Cu⁰ (Fig. 6b) nanoparticles.

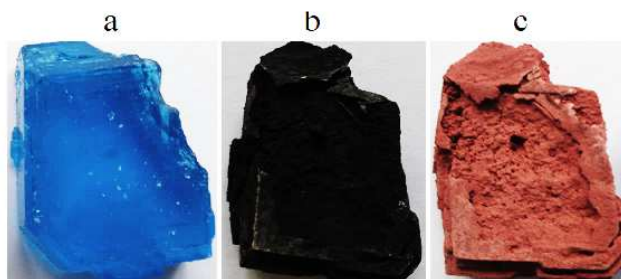


Fig. 4. Photographic images of freshly prepared crystal $\text{Cu}(\text{HCOO})_2 \cdot 4\text{H}_2\text{O}$ (a) and the products of its thermolysis in air (b) and in helium atmosphere (c) at $400\text{ }^\circ\text{C}$.

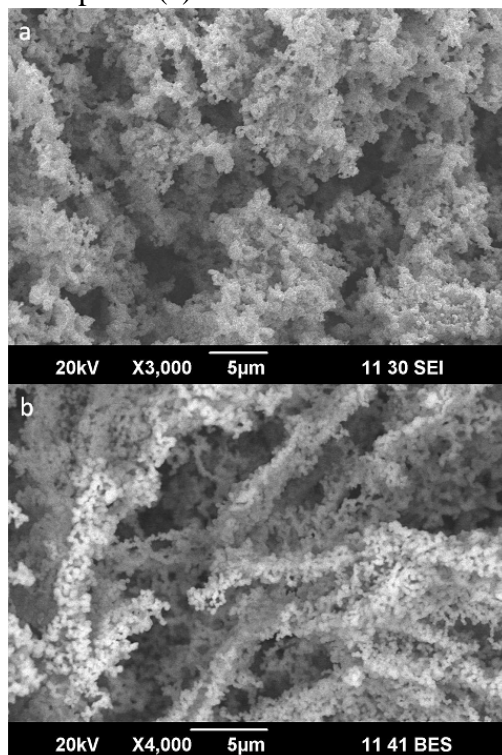


Fig. 5. SEM images of the morphology of the products of $\text{Cu}(\text{HCOO})_2 \cdot 4\text{H}_2\text{O}$ thermolysis in air (a) and in helium atmosphere (b) at $400\text{ }^\circ\text{C}$.

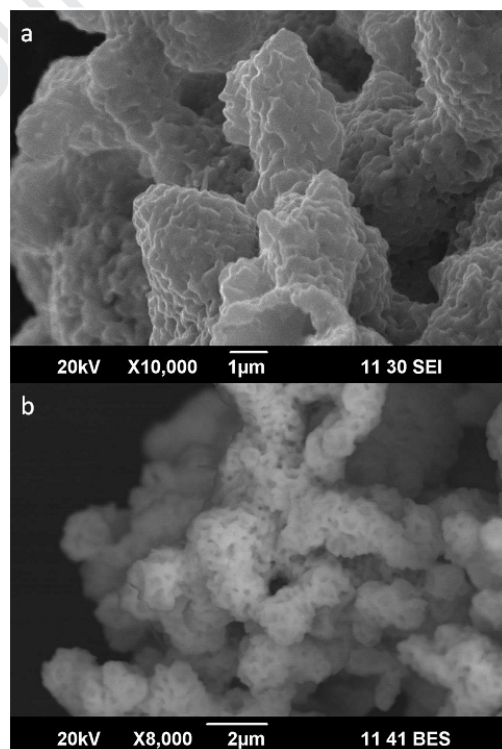


Fig. 6. SEM images of the morphology of the products of $\alpha\text{-Cu}(\text{HCOO})_2$ thermolysis in air (a) and in helium atmosphere (b) at $400\text{ }^\circ\text{C}$.

As seen from Fig. 7 and Table 1, the IR spectra of the orthorhombic (α) and monoclinic (β) structural modifications of anhydrous copper(II) formate are similar. The differences are in the splitting of some bands into two components in the IR spectrum of α -Cu(HCOO)₂. The absorption bands observed in the IR spectra of the compounds are typical of metal-coordinated ion HCOO⁻ [42]. A very intensive absorption band split into two components, 1606 and 1555 cm⁻¹, is responsible for the asymmetric stretching vibrations of C-O bonds of OCO group in the IR spectrum of α -Cu(HCOO)₂. Analogous vibrations of C-O bonds in the IR spectrum of β -Cu(HCOO)₂ are characterized by a very intensive band at 1566 cm⁻¹. A very intensive narrow band at 1396 (shoulder), 1361 cm⁻¹ (α) and 1367 cm⁻¹ (β) is responsible for the symmetric stretching vibrations of C-O bonds of OCO group. The stretching vibrations of C-H bonds manifest themselves as a weak broad band split into two components, 2998, 2925 cm⁻¹ (α) and 3000, 2924 cm⁻¹ (β). A very weak band with absorption maximum at 1052 cm⁻¹ (α) and 1063 cm⁻¹ (β) is responsible for the bending vibrations of C-H bonds. The narrow band of medium intensity at 819 cm⁻¹ (α), 821 cm⁻¹ (β) is due to the scissors vibrations of OCO [42]. The bands with absorption maxima at 436, 399 cm⁻¹ (α) and 426 cm⁻¹ (β) can be attributed to the stretching vibrations of Cu-O bonds [35,43]. The broad weak band at ~3500 cm⁻¹ observed on the IR spectra (Fig. 7) is related to the stretching vibrations of O-H bonds of sorbed H₂O molecules. This is confirmed by the fact that this band is absent on the IR (ATR) spectra (**Fig. 7S, Table 1S**).

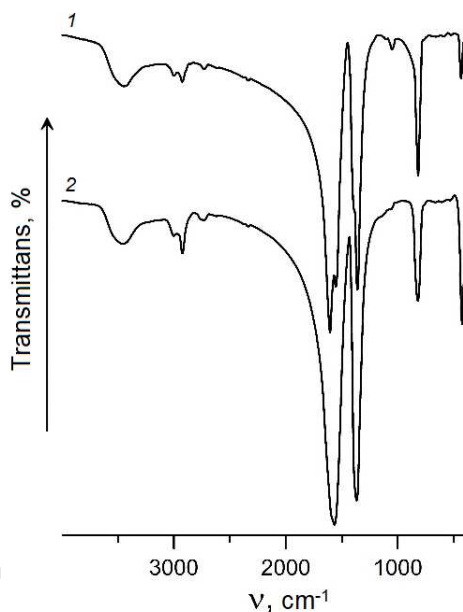


Fig. 7. IR spectra of α -Cu(HCOO)₂ (1) and β -Cu(HCOO)₂ (2).

Table 1. Assignment of bands in IR spectra of α and β modifications of Cu(HCOO)₂.

α -Cu(HCOO) ₂	β -Cu(HCOO) ₂	Assignment
2998	3000	ν C-H
2925	2924	
1606	1566	ν_{as} COO
1555		
1396 (sh.)	1367	ν_s COO
1361		
1052	1063	δ C-H
819	821	δ OCO
436	426	ν Cu-O
399		

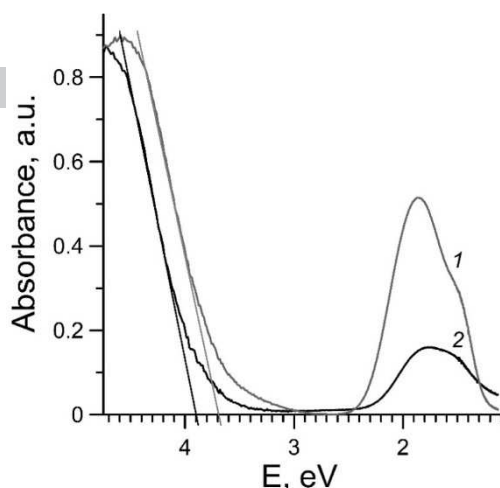


Fig. 8. UV-Vis-NIR spectra of α -Cu(HCOO)₂ (1) and β -Cu(HCOO)₂ (2).

The absorption spectra of anhydrous copper(II) formate samples were studied in UV, visible and NIR ranges (Fig. 8). In octahedral crystal field, the main electronic state for Cu²⁺ (d^9 (2D)) is $t_{2g}^6e_g^3$, which agrees with the term 2E_g . The term $^2T_{2g}$ corresponds to the excited electronic state $t_{2g}^5e_g^4$ [44]. In the octahedral crystal field of the β -Cu(HCOO)₂ there is only one electron transition $^2E_g \rightarrow ^2T_{2g}$ for Cu²⁺, which is observed in the absorption spectrum at 1.77 eV. Distortion of octahedron (by elongation or compression) leads to tetragonal symmetry. The ground state 2E_g is split due to the Jahn-Teller effect into $^2B_{1g}$ (becomes the ground state) and $^2A_{1g}$ states in tetragonal symmetry, which leads to symmetry reduction for Cu²⁺ ion. The excited term $^2T_{2g}$ is split into $^2B_{2g}$ and 2E_g states. In the absorption spectrum of the orthorhombic phase α -Cu(HCOO)₂, in whose structure the copper atoms are located in tetragonal pyramids CuO₅ [30], the bands typical of Cu²⁺ are registered: the band at 1.86 eV corresponds to $^2B_{1g} \rightarrow ^2E_g$ transition and the band at 1.48 eV – to $^2B_{1g} \rightarrow ^2B_{2g}$ transition. The values of the charge-transfer absorption band edge are 3.7 eV for α -Cu(HCOO)₂ and 3.9 eV for β -Cu(HCOO)₂.

The magnetic properties of anhydrous copper formate have long attracted the attention of researchers in connection with the problems of low-temperature magnetism and magnetic transitions in simple metal organic structures. It was shown [30] that α -Cu(HCOO)₂ above 20 K is a paramagnetic compound with Curie constant $C = 0.438$ and magnetic moment per copper ion $\mu = 1.87 \mu_B$. The paramagnetic Curie temperature Θ (Weiss constant), was evaluated as 9.8 K, indicative of a ferromagnetic transition. As distinct from the α phase, β -Cu(HCOO)₂ is ordered at a higher temperature (30.4 K), and in the ordered phase it exhibits a state attributed to weak ferromagnetism [32]. Our studies of the α and β modifications of anhydrous copper(II) formate confirmed that their magnetic behaviors differ considerably. From Fig. 9 it is seen that α -Cu(HCOO)₂ at ≈ 8.5 K undergoes a ferromagnetic ordering, the magnetization grows at this temperature by several orders of magnitude. The magnetization curve measured at 2 K reaches saturation in the field of 0.1 T. Extrapolation of the saturation area to zero field makes it possible to determine the magnetic moment value per copper ion. It is $1.1 \mu_B$, which confirms the conclusion about the ferromagnetic character of ordering in this phase [32,45], however, it is much lower than that obtained in these works at 5 and 7 K. From Fig. 9 it also follows that the magnetization of the ferromagnetic phase α -Cu(HCOO)₂ decreases abruptly when the temperature falls below 5 K. The nature of this effect requires special studies using magnetic neutron diffraction analysis methods. At temperatures above 25 K, α -Cu(HCOO)₂ behaves as a paramagnet; Figure 10 shows the temperature dependence of magnetic susceptibility measured in the 0.01 T field.

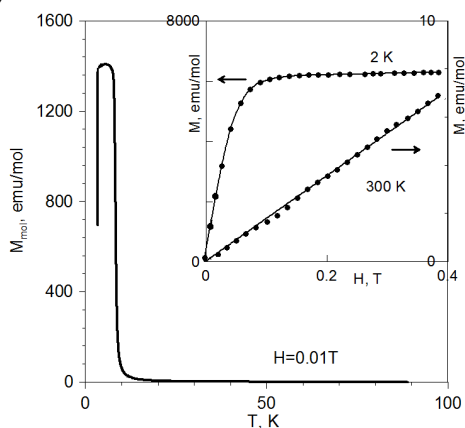


Fig. 9. Magnetization of α -Cu(HCOO)₂ vs temperature and magnetic field (inset).

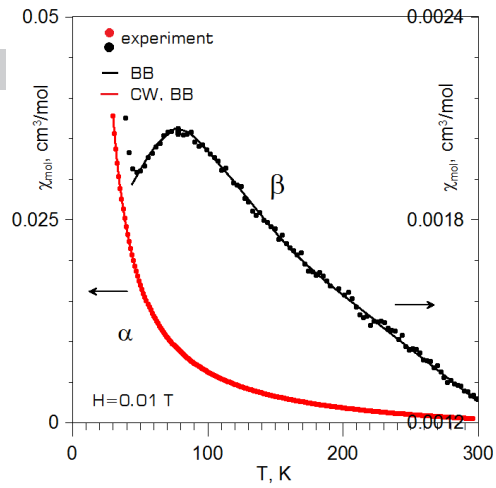


Fig. 10. Temperature dependences of magnetic susceptibility for α - and β -Cu(HCOO)₂.

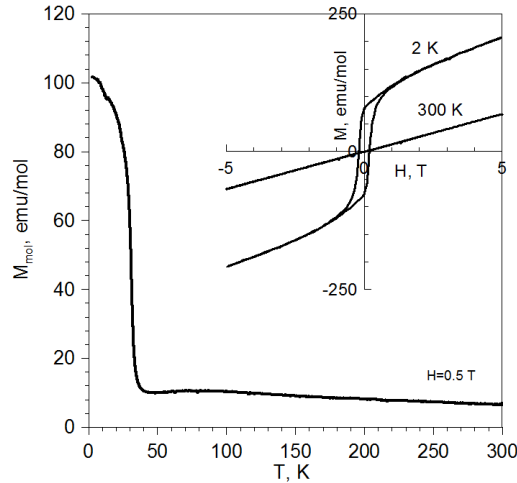


Fig. 11. Temperature and field (inset) dependences of magnetization for β -Cu(HCOO)₂.

The susceptibility of α -Cu(HCOO)₂ at $T > 25$ K is described well by the Curie-Weiss law $\chi = A + C/(T - \Theta)$ (CW), where A is the temperature-independent part including the diamagnetic correction and Van Vleck paramagnetism. Figure 10 displays the measured values of magnetic susceptibility and the result of their CW approximation. It is seen that the experimental and calculated data are in good agreement. The following values were obtained: $A = -0.0017$ cm³/mol, $C = 0.658$ cm³/mol*K, $\Theta = 15.8$ K ($R = 0.94$). A positive value of Θ is indicative of ferromagnetic exchange interactions between copper ions in α -Cu(HCOO)₂, which at low temperatures lead to ferromagnetic ordering. However, magnetic moment per copper ion calculated by formula $\mu = \sqrt{8C}$ is $2.29 \mu_B$. This is much larger than the spin-only value for the d^9 configuration, $S = 1/2$ ($1.0 \mu_B$). Overestimated values of magnetic moments are often observed for compounds containing Cu²⁺ cations [5]. They can be interpreted as a result of incomplete orbital moment quenching possible for this electronic configuration. On the other hand, it is known [32] that the structure of α -Cu(HCOO)₂ contains Cu-Cu dimers, which magnetically can be treated as exchange-coupled clusters, whose behavior is usually considered in the framework of the Heisenberg-Dirac-Van Vleck model. For the description of the temperature dependence of magnetic susceptibility, we used a particular case for dimer, the so-called Bleaney-Bowers equation: $\chi = N_A g^2 \beta^2 / 2 * 3k_B T * [1 + 1/3 \exp(-2J/k_B T)]^{-1} + A$ (BB), where J is an exchange interaction parameter in dimers and A (as in CW) is a temperature-independent part including the diamagnetic correction and Van Vleck paramagnetism. Fitting of the parameters J and A yielded $J = +16.9$ cm⁻¹ and $A = -0.0028$ cm³/mol ($R = 0.94$). The values of the R factor in the calculations by formulas (CW) and (BB) coincide, therefore the results of approximation in Fig. 10 also completely coincide. The values of the temperature-independent contribution to magnetic susceptibility obtained by two formulas are predictably similar. The obtained positive value of the exchange parameter demonstrates the reasonableness of the employed model. The ferromagnetic character of α -Cu(HCOO)₂ at low temperatures is in line with the results of first-principle modeling of electronic band structure discussed below.

β -Cu(HCOO)₂ exhibits magnetism of different character. Magnetic ordering of β -Cu(HCOO)₂ takes place at 30.5 K, which agrees well with data [32]. It is characterized by a rather large hysteresis (Fig. 11, inset).

Extrapolation of the field dependence of magnetization to zero field yields here $0.012 \mu_B$ moment per copper ion. This is two orders of magnitude smaller than in case of α -Cu(HCOO)₂. At higher temperatures for β -Cu(HCOO)₂, as distinct from α modification, a more complex dependence of magnetic susceptibility is observed. This dependence deviates considerably from the Curie-Weiss law: at ≈ 70 K a wide maximum is observed on the temperature dependences of susceptibility and magnetization (Figs. 10, 11). In work [46], the anomalies of this function are discussed in the framework of the antiferromagnetic Heisenberg model for spin $S = \frac{1}{2}$, allowing $\chi(T)$ to be expressed as a series in terms of powers of function $k_B T_c/J$. However, a more demonstrative and no less successful model is the BB model offering a good explanation of the $\chi(T)$ dependences with a broad maximum typical of exchange-coupled clusters with antiferromagnetic exchange. Using the (BB) equation for the description of susceptibility of β -Cu(HCOO)₂ at temperatures above 50 K, we have the value of exchange parameter $J = -39.4 \text{ cm}^{-1}$. The results of approximation are shown by a black solid line in Fig. 10. The negative sign of the exchange parameter confirms the antiferromagnetic bonding between copper ions in clusters. When the temperature decreases, a transition to antiferromagnetic state occurs (Fig. 11). The observed in [32] weak ferromagnetism, with very small values of copper magnetic moments, $0.06 \mu_B$, has then to be attributed to canting effect. The antiferromagnetic character of β -Cu(HCOO)₂ at low temperatures is confirmed by the first-principles calculations of the electronic band structure performed by the authors.

2. Electronic band structure and magnetism of α - and β -Cu(HCOO)₂

Formate α -Cu(HCOO)₂ crystallizes in orthorhombic structure $Pbca$, whose parameters are reported in [30], and β -Cu(HCOO)₂ – in monoclinic structure $P2_1/ac$ with parameters given in [32]. Figures 12 and 13 show the cells of these structures plotted with the use of the VESTA program [47], which for illustration purposes are doubly broadened in the b direction for α -Cu(HCOO)₂ and in the direction of c axis for β -Cu(HCOO)₂. The main structural elements of α -Cu(HCOO)₂ are edge-sharing tetragonal pyramids CuO₅ forming dimers. All 10 vertices of a dimer are connected with neighboring dimers through carboxylate groups.

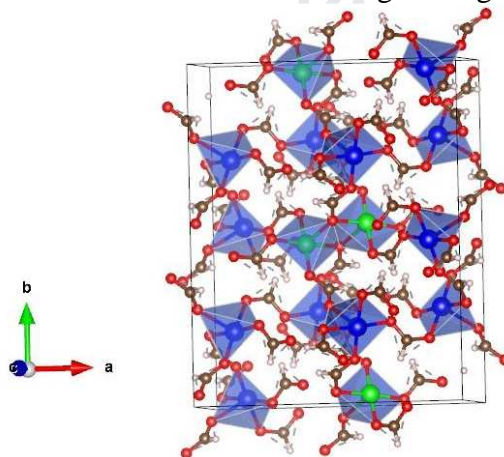


Fig. 12. Unit cell of α -Cu(HCOO)₂.

By contrast, the main structural elements of β -Cu(HCOO)₂ are distorted CuO₆ octahedra, each of which shares edges with two adjacent octahedra forming chains in the direction of the c axis. The neighboring chains are also connected with each other by formate groups. In the case of α -Cu(HCOO)₂, the electronic structure calculations were carried out for a primitive unit cell of atomic composition Cu₈O₃₂C₁₆H₁₆ with parameters reported in [30], whose dimensions are large enough for modeling both ferro- and antiferromagnetic ordering. The calculations have been performed for the totally ferromagnetic ordering of the copper magnetic moments, whereas for the antiferromagnetic ordering the opposite orientation of copper moments inside the adjacent pyramids of the dimers has been accepted. In the case of β -Cu(HCOO)₂, the calculations were performed for a doubled cell (Fig. 13) with atomic composition Cu₄O₁₆C₈H₈. Doubling in the c axis also makes it possible to model ferro- and antiferromagnetic ordering in the chains of octahedrons. For the ferromagnetic ordering the equal orientation of all the moments has been accepted whereas for the antiferromagnetic model the opposite orientation of the copper atoms moments nearest inside the chains was supposed. An important detail of the calculation is the choice for the initial magnetic moments of the self-consistency process. We have detected that taking these values less than $2 \mu_B$ we can achieve the self-consistent values of magnetic moment in good agreement with experiment data, $\sim 1 \mu_B$, whereas with higher initial moments the final moments are strongly overestimated.

The electronic band structure calculations were carried out using the pseudo-potential augmented projector waves (PAW) method of the electronic density functional theory as implemented in the Vienna ab-initio simulation package VASP [48]. Program supplied PAW-type atomic exchange-correlation potentials were used. The electronic band states were calculated on a grid containing 24 wave vectors per the irreducible part of the Brillouin zone in case of α -Cu(HCOO)₂ and 68 vectors in case of β -Cu(HCOO)₂. Band states wave functions were expanded in plane waves with energy cutoff 600 eV. The densities of band states were plotted using the energy level broadening of 0.05 eV.

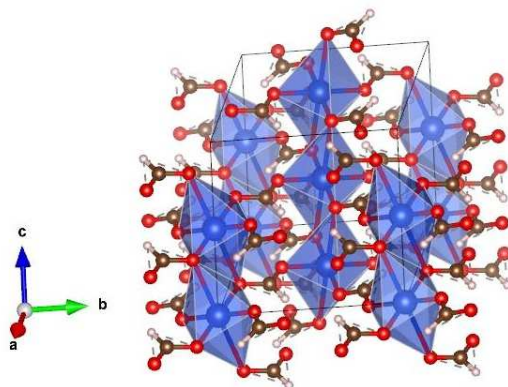


Fig. 13. Unit cell of β -Cu(HCOO)₂.

The known error of the computational methods based on the GGA approximation is underestimation of band gap in semiconductors containing d or f elements, which sometimes leads even to an incorrect character of conductivity. For copper oxides, the methods for elimination of this error were analyzed in greater detail in work [49]. It was shown that the effective method for band structure correction is the so-called GGA+U approximation, in which single-center Anderson exchange-correlation corrections are introduced for d or f states; the exchange corrections depend on the U parameter and the correlation correction – on the J parameter. The most frequently used version of GGA+U approximation is proposed by Dudarev et al. [50], in which corrections depend on the value of only one parameter U-J determining both exchange and correlation. For copper oxides it was shown [49] that the optimal value is $U-J = 7.5-0.98$ eV; this value of parameter U-J was used as a standard value also in works [51-53].

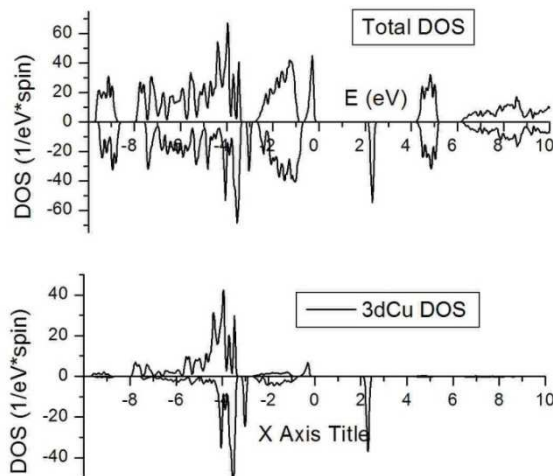


Fig. 14. Total and 3d Cu densities of states for ferromagnetic α -Cu(HCOO)₂ phase in GGA+U approximation with $U-J=6.5$ eV. The Fermi level counts as the zero of energy. The sign of the DOS,s corresponds to sign of the z spin projection.

We analyzed the effectiveness of application of the GGA+U and GGA approximations to copper formates. Figure 14 displays the total and 3dCu densities of states (DOS) for α -Cu(HCOO)₂ in the case of GGA+U approximation at $U-J = 6.5$ eV. Comparison of the total and partial DOS shows that the occupied 3dCu states with the positive spin projection are located in the interval from -6 to -3 eV, the states with the negative spin projection have the energy between -4.5 and -3 eV, and the empty states with the negative spin have the energy of about 2.2 eV. It follows that the minimal excitation energy between copper states is about 5 eV, which does

not agree with our absorption spectra indicating that the maximal energy of transitions between 3d states does not exceed ~ 2.5 eV ($\lambda \sim 400$ nm).

In order to evaluate the application efficiency of the GGA+U approach at small values of U, we also calculated optical absorption for the ferromagnetic α -Cu(HCOO)₂. According to the theory [54], the absorption coefficient, determined as reduction of electric vector of light wave per a unit of propagation length in crystal, depends mostly on the imaginary part of the dielectric function ϵ_2 . In Fig. 15, the function ϵ_2 calculated by using the GGA and GGA+U approximations with U-J = 1 and 2 eV and the corresponding absorption coefficient K are compared with our experimental data. In the experimental spectrum, the interval from 1 to 2.5 eV corresponds to transitions between 3d states of copper, and fundamental absorption begins at energies above 3 eV. In the GGA approximation, the 3dCu excitations are also within the interval 1 – 2.5 eV. The introduction of exchange-correlation corrections leads to a considerable increase of the energy of 3dCu excitations, at U-J = 2 eV the band of 3dCu excitations merges with the band of fundamental excitations, which does not agree with the experimental data.

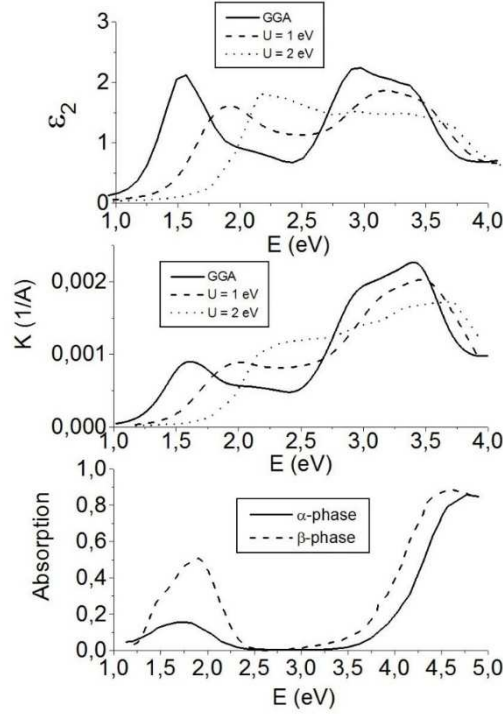


Fig. 15. The calculated values of the imaginary part of dielectric function ϵ_2 , absorption coefficient K , and experimental absorption coefficient for α - and β -Cu(HCOO)₂.

Thus, at any values of U-J parameter, the description of the low-temperature excitation spectrum on the basis of GGA+U calculations is likely to be worse than in the “classical” GGA approach. The total DOS in the GGA approximation for ferromagnetic α -modification of Cu(HCOO)₂ and several partial DOS's are given in Fig. 16. The states in the vicinity of -10 eV are built mainly of hydrogen 1s orbitals. Above them, in the interval from -8.5 to -5 eV, weakly spin-polarized hybrid states built of almost similar contributions of $2p_{O_{pl}}$ and $2p_{C_{pl}}$ orbitals are located, where O_{pl} are atoms making up square bases of pyramidal clusters CuO_4 and C_{pl} are atoms of formate groups coupled with O_{pl} atoms (we omit the discussion of DOS's of oxygen atoms forming vertices of pyramids and coupled with them carbon atoms since they differ insignificantly from analogous DOS in Fig. 16). Similarly, there are strongly hybridized $2p_{O_{pl}}-2p_{C_{pl}}$ states above the Fermi level at energy of about 4 eV. It follows then that the states between -8.5 and -5 eV are bonding oxygen-carbon states and at about 4 eV are their antibonding counterparts. In the range from -4.5 eV to the Fermi level, the bands of $2p_{O_{pl}}$ states that are not hybridized with the states of carbon atoms, i.e. nonbonding states of formate groups, are located. Above this group of states, from -2 eV to the Fermi level and over it, there are 3dCu states, which are also partially hybridized with the 2p states of O_{pl} atoms. The density of $2p_{O_{pl}}$ states is relatively small, however, because of their large number they considerably contribute to the cell magnetization. Near the Fermi level there are two $3d_{x^2-y^2}$ states, one occupied and one empty, with the energy interval between them equal to 1.1 eV, corresponding to exchange splitting. From the shape of the band structure it follows that copper atoms have the electron configuration $Cu 3d^9$ and magnetic moment close to $1 \mu_B$, which corresponds to our experimental estimates of copper magnetic moment, $1.1 \mu_B$, and differs considerably from the estimates of work [30]. The

calculations also show that the lower fundamental absorption edge at energy above 3 eV corresponds to transitions from the 3d states of copper to the 2p states of carbon.

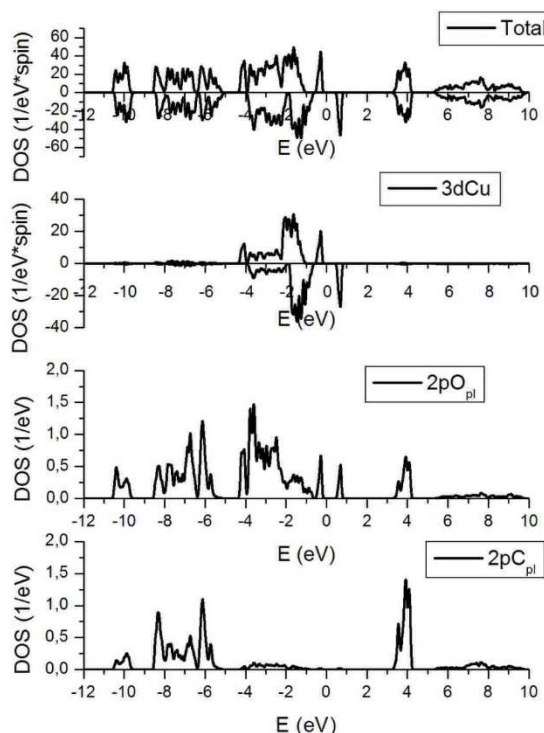


Fig. 16. Total and partial densities of states for ferromagnetic α -modification of $\text{Cu}(\text{HCOO})_2$ in GGA approximation. The Fermi level counts as the zero of energy. Total and 3dCu DOS are given for positive and negative spin projections, and DOS summed over spin projections are presented for oxygen and carbon atoms.

Such calculations for *ferromagnetic* ordering in β - $\text{Cu}(\text{HCOO})_2$ yield the densities of states close to the DOS of α - $\text{Cu}(\text{HCOO})_2$; this contradicts the results of work [32] pointing to small values of magnetic moments for this phase, $0.066 \mu_B$, which according to our data are $0.012 \mu_B$. Hence, in accordance with our measurements, β - $\text{Cu}(\text{HCOO})_2$ at low temperatures is likely to be antiferromagnetic, and small values of its magnetic moments are due to the *canting* effect at small deviations of the direction of magnetic moments from the axis of their antiferromagnetism. For β - $\text{Cu}(\text{HCOO})_2$, 2 models of antiferromagnetic ordering are possible. In the first, the antiferromagnetic ordering can take place inside chains of copper-oxygen octahedra, while in the second model the ordering inside the chains is ferromagnetic, but the directions of magnetic moments in the neighboring chains are antiparallel. Some characteristics of the electronic structure of α - and β - $\text{Cu}(\text{HCOO})_2$ obtained from the GGA approximation calculations are listed in Table 2.

Table 2. The characteristics of the band structure and magnetism in α and β phases of $\text{Cu}(\text{HCOO})_2$

Characteristic	α phase	β phase
Band gap (eV)	3.34 (3.70)*	3.58 (4.01)
Experimental band gap (eV)	3.67	3.87
Magnetic moment of copper atom (μ_B)	0.59	0.54
Total energy (E_{fm}) of ferromagnetic cell (eV)	-446.281	-222.765
Total energy (E_{afm}) of antiferromagnetic cell (eV)	-446.264	-222.949 (-221.864)**

*Band gap in GGA+U approximation at U-J=1 eV.

**Total energy value for the second model of antiferromagnetic ordering.

It follows that the GGA approach leads as usual to an underestimated value of the fundamental absorption onset energy; however, such calculations correctly reproduce the increase of the fundamental absorption edge from α to β modification of anhydrous copper(II) formate. Note that the introduction of exchange-correlation corrections in the GGA+U approximation at small U values leads only to partial improvement: for α - $\text{Cu}(\text{HCOO})_2$ the calculated energy gap width corresponds better to the experimental value, but for β -

Cu(HCOO)₂ it is overestimated. A lower energy E_{fm} of ferromagnetic cell of α -Cu(HCOO)₂ corresponds to experimentally observed ferromagnetism, whereas a lower value of E_{afm} for the antiferromagnetic cell of β -Cu(HCOO)₂ corresponds to a very small experimental value of copper magnetic moment. Moreover, the difference $E_{fm}-E_{afm}$, -0.0217 eV for α -Cu(HCOO)₂ and 0.184 eV for β -Cu(HCOO)₂, in accordance with experiment, is indicative of a higher value of the critical temperature for β modification of copper(II) formate. In the case of β -Cu(HCOO)₂, the total energy value for the first model of antiferromagnetism turns out to be much smaller than that for the second model. We conclude then that the antiferromagnetic ordering in β -Cu(HCOO)₂ at $T < 9$ K is probably realized along the octahedra chains. This result contradicts the data of the work [32] offering analysis of magnetism above 9 K, in which it is concluded that weak ferromagnetic ordering is realized in the paramagnetic region inside the chains, whereas antiferromagnetic ordering occurs between the chains. However, our theoretical conclusions on the nature of antiferromagnetism agree with our results of modeling the temperature dependence of susceptibility based on the antiferromagnetic ordering in the chains. Note also that the doubled value of the total energy for the first model of antiferromagnetic cell of β -Cu(HCOO)₂, -445.898 eV, is higher than the total energy for α -Cu(HCOO)₂. Consequently, the β modification of Cu(HCOO)₂ is metastable, which agrees with both our observations and the results of work [32], bearing witness to slow transformation of β -Cu(HCOO)₂ into α -Cu(HCOO)₂ during weak heating.

A certain disagreement with the experimental data lies in the fact that for a ferromagnetic cell of α -Cu(HCOO)₂ the calculated magnetic moment of the copper atom, 0.59 μ_B , is smaller than our experimental value, 1.1 μ_B , and besides it does not correspond to the conclusions following from analysis of the densities of states. However, this contradiction can be explained based on the effect of magnetization delocalization throughout the cell. The calculations show that all oxygen atoms have the same spin polarization direction as copper atoms. Their magnetic moment values are small, from 0.07 to 0.1 μ_B , but together they make a considerable contribution to magnetization. Since the experimental value of copper atom magnetic moment is found from magnetization values of the whole cell, then referring our estimated value of magnetization of the whole cell of α -Cu(HCOO)₂, 7.64 μ_B , to copper atoms, we have $M(\text{Cu}) = 0.95 \mu_B$, in good agreement with the experiment.

Conclusion

Thus, as a result of the studies performed we have developed a universal technique for the synthesis of anhydrous copper(II) formate in the form of orthorhombic (α) and monoclinic (β) modifications, as well as dehydrate and tetrahydrate. The technique is based on the interaction of copper(II) nitrate with formic acid, which is represented in the form of two possible reactions (1 and 2). The structure and composition of the synthesized compound were specified by varying the concentration of formic acid, temperature and crystallization conditions. Reaction (1) is possible only when Cu(NO₃)₂·3H₂O is dissolved in concentrated formic acid; reaction (2) is more environmentally friendly since it proceeds without emission of toxic NO₂ vapors, however, in that case much more formic acid and water are consumed. Moreover, reaction (2) is specific for solving the problem of synthesis of Cu(HCOO)₂·2H₂O and Cu(HCOO)₂·4H₂O hydrates.

One of the most important properties of compounds of the general composition Cu(HCOO)₂·nH₂O is their ability to transform into Cu⁰ metal during heating in inert atmosphere, which can be used for producing copper contacts, powders and composites based thereon. In this respect, of much interest is tetrahydrate, the thermolysis of which leads to the production of copper powder with particle size of the order of 150 nm.

The obtained temperature dependences of magnetization of anhydrous modifications of Cu(HCOO)₂ are described well in the framework of the Bleaney-Bowers model. The values of critical temperatures found in this model correspond to low-temperature ferromagnetic ordering of α -Cu(HCOO)₂ and antiferromagnetic ordering of β -Cu(HCOO)₂. For α modification, the magnetic moment values obtained from the BB model increase appreciably with a rise in temperature from 1 to 7 K, which is probably due to the known effect of orbital moments tempering.

For the electronic band structure modeling we tested two approaches: the GGA+U approximation usually used for the calculation of the band structure of copper oxides and the “classical” GGA approximation for exchange-correlation potential. It was shown that a more correct description of absorption spectra is achieved in the GGA approximation, whereas the GGA+U approach is inadequate since absorption between copper ion terms is superimposed on the fundamental absorption with charge transfer. The GGA approach indicates that absorption with charge transfer takes place between the band states of copper and carbon atoms; this approach describes correctly the increase of the edge of this adsorption from α to β modification. On the other hand, the GGA approach gives a description of low-temperature magnetic ordering corresponding to the results of our experiments. For β -Cu(HCOO)₂, the modeling indicates an antiferromagnetic ordering of moments in chains of

copper-oxygen octahedra, in agreement with the Bleaney-Bowers model. A higher calculated value of the total energy for β -Cu(HCOO)₂ suggests the instability of this structural modification compared with α -Cu(HCOO)₂, which also agrees with the experimental data.

Acknowledgment

This work was carried out in accordance with the scientific and research plans and state assignment of the Institute of Solid State Chemistry of the Ural Branch of the Russian Academy of Sciences (grant No. AAAA-A19-119031890025-9). The UV-Vis spectra were recorded on equipment of the Center for Joint Use "Spectroscopy and Analysis of Organic Compounds" at the Postovsky Institute of Organic Synthesis, UB RAS. The calculations were performed in URAN cluster at the Institute of Mathematics and Mechanics, UB RAS. E.V.C. acknowledges support from the Saint Petersburg State University (Grant No. 51126047) and Tomsk State University competitiveness improvement programme (project 8.1.01.2018).

Conflict of Interest

The authors declare that they have no conflict of interest.

All authors made substantial contributions to the conception of the work, analysis and interpretation of data, and drafted the work and revised it critically for important intellectual content. Material preparation, data collection and analysis were performed by [V.P. Zhukov], [E.V. Chulkov], [I.V. Baklanova], [D.G. Kellerman], [O.I. Gyrdasova], [T.V. Dyachkova] and [A.P. Tyutyunnik]. The first draft of the manuscript was written by [V.N. Krasil'nikov] and all authors commented on previous versions of the manuscript. All authors read and approved the final manuscript.

References

1. K.L. Hu, M. Kurmoo, Z. Wang, S. Gao, Metal-organic perovskites: synthesis, structures, and magnetic properties of [C(NH₂)₃] [MII(HCOO)₃] (M = Mn, Fe, Co, Ni, Cu, and Zn; C(NH₂)₃ = guanidinium), *Chem. Eur. J.* 15 (2009) 12050-12064. DOI: 10.1002/chem.200901605.
2. Z. Wang, P. Jain, K.Y. Choi, J. van Tol, A.K. Cheetham, H.W. Kroto, H.J. Koo, H. Zhou, J. Hwang, E.S. Choi, M.H. Whangbo, N.S. Dalal, Dimethylammonium copper formate [(CH₃)₂NH₂]Cu(HCOO)₃: A metal-organic framework with quasi-one-dimensional antiferromagnetism and magnetostriction, *Phys. Rev. B.* 87 (2013) 224406. DOI: 10.1103/PhysRevB.87.224406.
3. P. Samarasekere, X. Wang, A.J. Jacobson, J. Tapp, A. Moller, Synthesis, crystal structures, magnetic, and thermal properties of divalent metal formate-formamide layered compounds, *Inorg. Chem.* 53 (2014) 244-256. doi.org/10.1021/ic402200v.
4. B. Pato-Doldan, L.C. Gomez-Aguirre, A.P. Hansen, J. Mira, S. Castro-Garcia, M. Sanchez-Andujar, M.A. Senaris-Rodríguez, V. Zapf, J. Singleton, Magnetic transitions and isotropic versus anisotropic magnetic behaviour of [CH₃NH₃][M(HCOO)₃] M = Mn²⁺, Co²⁺, Ni²⁺, Cu²⁺ metal-organic perovskites, *J. Mater. Chem. C* 4 (2016) 11164-11172. DOI: 10.1039/c6tc03992h.
5. S.M. Bovill, R.J.C. Dixey, P.J. Saines, Three coordination frameworks with copper formate based low dimensional motifs: synthesis, structure and magnetic properties, *CrystEngComm.* 19 (2017) 1831-1838. DOI: 10.1039/c6ce01601d.
6. I.E. Collings, M. Bykov, E. Bykova, M. Hanfland, S. van Smaalen, L. Dubrovinsky, N. Dubrovinskaia, Disorder-order transitions in the perovskite metalorganic frameworks [(CH₃)₂NH₂][M(HCOO)₃] at high pressure, *CrystEngComm.* 20 (2018) 3512-3521. DOI: 10.1039/C8CE00617B.
7. V. Rosenband, A. Gany, Preparation of nickel and copper submicrometer particles by pyrolysis of their formates, *J. Mater. Proc. Technol.* 153-154 (2004) 1058-1061. http://dx.doi.org/10.1016%2Fj.jmatprotec.2004.04.165.
8. V.N. Krasil'nikov, V.V. Antsygina, G.V. Bazuev, Chem. Inform. Abstract: Synthesis of Bi_{2-x}Pb_xSr₂Ca₂Cu₃O₁₀ from formates. Volume 26, Issue 49 December 5, 1995. https://doi.org/10.1002/chin.199549010. (*Zhurnal Neorganicheskoi Khimii* 40 (1995) 1065-1069).
9. B. Nakhjavan, M.N. Tahir, M. Panthofer, H. Gao, T.D. Schladt, T. Gasi, V. Ksenofontov, R. Branscheid, S. Weber, U. Kolb, L.M. Schreiber, W. Tremel, Synthesis, characterization and functionalization of nearly mono-disperse copper ferrite Cu_xFe_{3-x}O₄ nanoparticles, *J. Mater. Chem.* 21 (2011) 6909-6915. DOI: 10.1039/c0jm04577b.

10. O.I. Gyrdasova, M.A. Melkozerova, I.V. Baklanova, L.Yu. Buldakova, N.S. Sycheva, V.N. Krasil'nikov, M.Yu. Yanchenko, Synthesis, structure, optical and photocatalytic properties of copper-activated ZnO, *Mendelev Commun.* 27 (2017) 410-412. DOI: 10.1016/j.mencom.2017.07.031.
11. J. Hwang, S. Kim, K.R. Ayag, H. Kim, Copper electrode material using copper formate-bicarbonate complex for printed electronics, *Bull. Korean Chem. Soc.* 35 (2014) 147-150. <http://dx.doi.org/10.5012/bkcs.2014.35.1.147>.
12. P. Sun, S. Wang, Y. Li, T. Zhang, Supercritical hydrothermal synthesis of ultra-fine copper particles using different precursor, *Key Eng. Mater.* 744 (2017) 493-497. DOI:10.4028/www.scientific.net/KEM.744.493.
13. J. Lee, B. Lee, S. Jeong, Y. Kim, M. Lee, Microstructure and electrical property of laser-sintered Cu complex ink, *Appl. Surface Sci.* 307 (2014) 42-45. <http://dx.doi.org/10.1016/j.apsusc.2014.03.127>.
14. S. Kubota, T. Morioka, M. Takesue, H. Hayashi, M. Watanabe, R.L. Smith, Continuous supercritical hydrothermal synthesis of dispersible zero-valent copper nanoparticles for ink applications in printed electronics, *J. of Supercritical Fluids* 86 (2014) 33-40. <http://dx.doi.org/10.1016/j.supflu.2013.11.013>.
15. Y. Li, T. Qi, Y. Cheng, F. Xiao, A new copper ink with low sintering temperature for flexible substrates, 2015 16th International Conference on Electronic Packaging Technology (ICEPT) 11-14 Aug. 2015, 848-851. <https://doi.org/10.1109/ICEPT.2015.7236713>.
16. Y.S. Rosen, S. Magdassi, Effect of carboxylic acids on reactive transfer printing of copper formate ink, *MRS Advances* © 2018 Mater. Res. Soc. 3 (2018) 261-267. DOI: 10.1557/adv.2018.21.
17. C. Paquet, T. Lacelle, B. Deore, A.J. Kell, X.Y. Liu, I. Korobkov, P.R.L. Malenfant, Pyridine-copper (II) formates for the generation of high conductivity copper films at low temperatures, *Chem. Commun.* 52 (2016) 2605-2608. DOI: 10.1039/C5CC07737K
18. L.L.L. Sousa, G.F. Barbosa, F.L. A. Machado, L.R.S. Araujo, P. Brandao, M.S. Reis, D.L. Rocco, Magnetic dimensionality of metal formate $M[(H_2O)_2(HCOO)_2]$ compounds ($M = Co(II), Cu(II)$), *IEEE Transactions on Magnetics* 49 (2013) 5610-5615. DOI: 10.1109/TMAG.2013.2278681.
19. W. Fujita, Crystal structures, and magnetic and thermal properties of basic copper formates with twodimensional triangular-lattice magnetic networks, *RSC Adv.* 8 (2018) 32490-32496. DOI: 10.1039/c8ra07134a.
20. A.K. Galwey, D.M. Jamieson, M.E. Brown, Thermal decomposition of three crystalline modifications of anhydrous copper(II) formate, *J. Phys. Chem.* 78 (1974) 2664-2670. <https://doi.org/10.1021/j100619a006>.
21. M.A. Mohamed, A.K. Galwey, S.A. Halawy, Kinetic and thermodynamic studies of the nonisothermal decomposition of anhydrous copper(II) formate in different gas atmospheres, *Thermochim. Acta* 411 (2004) 13-20. DOI: 10.1016/j.tca.2003.07.003.
22. M.E. Brown, Thermal decomposition of copper(II) squarate, *J. Chem. Soc. Faraday Trans I*, 84 (1988) 1349-1356. DOI 10.1039/F19888401349.
23. N.J. Carr, A.K. Galwey, The thermal decomposition reactions of copper(II) maleate and of copper(II) fumarate, *J. Chem. Soc., Faraday Trans. I*, 84 (1988) 1357-1373. DOI: 10.1039/F19888401357.
24. A.K. Galwey, M.A. Mohamed, A kinetic and mechanistic study of the thermal decomposition of copper(II) mellitate, *Thermochim. Acta* 239 (1994) 211-224. doi:10.1016/0040-6031(94)87068-3
25. L.I. Yudanova, V.A. Logvinenko, N.F. Yudanov, N.A. Rudina, A.V. Ishchenko, P.P. Semyannikov, L.A. Sheludyakova, N.I. Alferova, I.V. Korol'kov, Preparation of a copper-polymer composite through the thermolysis of copper(II) succinate, *Inorg. Mater.* 50 (2014) 945-950. DOI: 10.1134/S0020168514090180.
26. D.A. Pomogailo, L.A. Petrova, D.A. Pomogailo, E.I. Knerelman, A.M. Kolesnikova, S.V. Barinov, K.A. Kydralieva, G.I. Dzhardimalieva, The structure and thermal properties of nanocomposites based on copper nanoparticles in a polyethylene matrix, *Nanosci. Technol.: Intern. J.* 8 (2017) 27-40. <https://www.researchgate.net/publication/317135449>.
27. D. Mott, J. Galkowski, L. Wang, J. Luo, C.J. Zhong, Synthesis of size-controlled and shaped copper nanoparticles, *Langmuir* 23 (2007) 5740-5745. <https://doi.org/10.1021/la0635092>.
28. T.F. Pascher, M. Oncak, C. van der Linde, M.K. Beyer, Release of formic acid from copper formate: hydride, proton-coupled electron and hydrogen atom transfer all play their role, *Chem. Phys. Chem.* 20 (2019) 1420-1424. DOI: 10.1002/cphc.201900095.
29. R.L. Martin, H. Waterm, Magnetic studies with copper(II) salts. Part I V.I Remarkable magnetic behaviour of copper(II) formate and its hydrates, *J. Chem. Soc.* 1959, 1359-1370. DOI: 10.1039/JR9590001359.
30. N. Burger, H. Fuess, Crystal structure and magnetic properties of copper formate anhydrate $\alpha-Cu(HCOO)_2$, *Solid State Commun.* 34 (1980) 699-703. [https://doi.org/10.1016/0038-1098\(80\)90959-X](https://doi.org/10.1016/0038-1098(80)90959-X).

31. K. Yamagata, Y. Kozuka, T. Morita, Magnetization process of nearly 2-dimensional $\text{Cu}(\text{HCOO})_2 \cdot 4\text{H}_2\text{O}$ and $\text{Cu}(\text{HCOO})_2 \cdot 2(\text{NH}_2)_2\text{CO}$. II Estimation of magnetic parameters, *J. Phys. Soc. Japan* 50 (1981) 421-425. <https://doi.org/10.1143/JPSJ.50.421>.
32. F. Sapina, M. Burgos, E. Escriva, J.V. Folgado, D. Marcos, A. Beltrh, D. Beltrh, Ferromagnetism in the α and β polymorphs of anhydrous copper(II) formate: two molecular-based ferromagnets with ordering temperatures of 8.2 and 30.4 K, *Inorg. Chem.* 32 (1993) 4337-4344. <https://doi.org/10.1021/ic00072a029>.
33. N. Narsimlu, K.S. Kumar, G.S. Sastry, Charge carrier transport in $\text{Cu}(\text{COOH})_2$ organic molecular single crystal, *Mater. Sci. Eng.: B* 40 (1996) 203-205. [https://doi.org/10.1016/0921-5107\(96\)01597-8](https://doi.org/10.1016/0921-5107(96)01597-8).
34. M. Bukowska-Strzyzewska, The crystal structure of copper(II) formate dihydrate, *Acta Cryst.* 19 (1965) 357-362. <https://doi.org/10.1107/S0365110X65003456>.
35. A.M. Heyns, The vibrational spectra of the copper(II) formates: Part II. The internal formate and lattice modes of $\text{Cu}(\text{HCOO})_2 \cdot 2\text{H}_2\text{O}$, *J. Mol. Struct.* 127 (1985) 9-20. [https://doi.org/10.1016/0022-2860\(85\)80146-0](https://doi.org/10.1016/0022-2860(85)80146-0).
36. J. Guo, J. Zhang, T. Zhang, R. Wu, W. Yu, Thermal decomposition mechanisms of a three-dimensional framework coordination polymer $[\text{Cu}(\text{HCOO})_2(\text{H}_2\text{O})_2]_\infty$, *Acta Phys. -Chim. Sin.* 22 (2006) 1206-1211. [https://doi.org/10.1016/S1872-1508\(06\)60055-7](https://doi.org/10.1016/S1872-1508(06)60055-7).
37. R. Kiriyama, H. Ibamoto, K. Matsuo, The crystal structure of cupric formate tetrahydrate $\text{Cu}(\text{HCOO})_2 \cdot 4\text{H}_2\text{O}$, *Acta Cryst.* 7 (1954) 482-483. <https://doi.org/10.1107/S0365110X54001521>.
38. J.R. Gunter, The crystal structure of topotactically dehydrated copper(II) formate tetrahydrate, *J. Solid State Chem.* 35 (1980) 43-49. [https://doi.org/10.1016/0022-4596\(80\)90461-2](https://doi.org/10.1016/0022-4596(80)90461-2).
39. N. Herres, H. Klapper, X-ray topographic study of the antiferroelectric phase transition and antiphase boundaries in copper formate tetrahydrate, *Z. Kristallogr.* 230 (2015) 677-688. DOI: 10.1515/zkri-2015-1853.
40. A. Garron, F. Epron, Use of formic acid as reducing agent for application in catalytic reduction of nitrate in water, *Water Research* 39 (2005) 3073-3081. doi:10.1016/j.watres.2005.05.012.
41. H. Langfelderova, O. Hodura, The relationship between the structures of Cu(II) complexes and their chemical transformations, *J. Thermal Anal.* 36 (1990) 1009-1023. <https://doi.org/10.1007/BF01904637>.
42. K. Nakamoto, *Infrared and Raman Spectra of Inorganic and Coordination Compounds. Part B: Applications in Coordination, Organometallic, and Bioinorganic Chemistry.* Wiley, New York (2009) 400 Pages. ISBN: 978-0-471-74493-1.
43. R.S. Krishnan, P.S. Ramanujam, Raman and infrared spectra of copper formate tetrahydrate, *Spectrochim Acta* 28A (1972) 2227-2231. [https://doi.org/10.1016/0584-8539\(72\)80196-X](https://doi.org/10.1016/0584-8539(72)80196-X).
44. R.J.D. Tilley, *Colour and the Optical Properties of Materials* John Wiley & Sons, 2020, 608 pp. (p. 296).
45. A. Gupta (ed.), *Magnetic Properties of Paramagnetic Compounds, Subvolume C*, Springer-Verlag Berlin Heidelberg 2017. DOI: 10.1007/978-3-662-49202-4.
46. L.J. de Jongh (ed), *Magnetic Properties of Layered Transition Metal Compounds*, Springer Netherlands, Dordrecht, 1990. <https://doi.org/10.1007/978-94-009-1860-3>.
47. K. Momma, F. Izumi, VESTA: a three-dimensional visualization system for electronic and structural analysis, *J. Appl. Crystallogr.* 41 (2008) 653-658. <https://doi.org/10.1107/S0021889808012016>.
48. G. Kresse, M. Marsman, J. Furthmüller, Vienna ab-initio simulation package. VASP the guide, (2018). <https://cms.mpi.univie.ac.at/vasp/vasp/vasp.html>.
49. M. Heinemann, B. Eifert, C. Heiliger, Band structure and phase stability of the copper oxides Cu_2O , CuO , and Cu_4O_3 , *Phys. Rev. B.* 87 (2013) 115111. <https://doi.org/10.1103/PhysRevB.87.115111>.
50. S.L. Dudarev, G.A. Botton, S.Y. Savrasov, C.J. Humphreys, A.P. Sutton, Electron-energy-loss spectra and the structural stability of nickel oxide: An LSDA+U study, *Phys. Rev. B.* 57 (1998) 1505-1509. <https://doi.org/10.1103/PhysRevB.57.1505>.
51. D. Wu, Q. Zhang, M. Tao, LSDA + U study of cupric oxide: Electronic structure and native point defects, *Phys. Rev. B.* 73 (2006) 235206. <https://doi.org/10.1103/PhysRevB.73.235206>.
52. L. Debbichi, M.C.M. de Lucas, P. Krüger, Electronic structure, lattice dynamics and thermodynamic stability of paramelaconite Cu_4O_3 , *Mater. Chem. Phys.* 148 (2014) 293-298. <https://doi.org/10.1016/j.matchemphys.2014.07.046>.
53. M. Forti, P. Alonso, P. Gargano, G. Rubiolo, Transition Metals Monoxides. An LDA+U Study, *Proc. Mater. Sci.* 1 (2012) 230-234. <https://doi.org/10.1016/j.mspro.2012.06.031>.
54. J.M. Ziman, *Principles of the Theory of Solids*, 1st edition, Cambridge University, 1964.

Highlights

A new method has been developed to produce different types of copper (II) formates.

Magnetic properties of α and β modifications of $\text{Cu}(\text{HCOO})_2$ are very different.

Electronic structure of α - and β - $\text{Cu}(\text{HCOO})_2$ is investigated using first-principle calculations.

Journal Pre-proof

Declaration of interests

The authors declare that they have no known competing financial interests or personal relationships that could have appeared to influence the work reported in this paper.

The authors declare the following financial interests/personal relationships which may be considered as potential competing interests:

Inna Baklanova, on behalf of the authors*

* Corresponding author: Dr. Inna Baklanova,
Institute of Solid State Chemistry, Ural Branch, Russian Academy of Sciences,
620990, Ekaterinburg, Russia
E-mail: baklanova_i@ihim.uran.ru

Ekaterinburg, Russia
April 8, 2020